Research Task

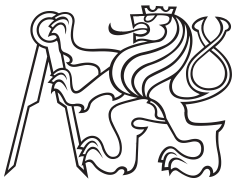

Czech Technical University in Prague

F4

Faculty of Nuclear Sciences and Physical Engineering
Department of Physics

Systematic study of impact of swept edge plasma potential biasing on turbulence in tokamaks

Filip Papoušek

Supervisor: Ing. Ondřej Grover
Field of study: Physics and Technology of Thermonuclear Fusion
September 2020

Acknowledgements

Děkuji svému vedoucímu za neutuchající podporu a užitečné rady. Dále děkuji týmům tokamaků COMPASS a GOLEM, že mi umožnily pracovat na mém výzkumném úkolu.

Declaration

Prohlašuji, že jsem předloženou práci vypracoval samostatně, a že jsem uvedl veškerou použitou literaturu.

V Praze, 15. September 2020

Contents

Figures

Introduction

In the tokamak plasma the edge plasma is the barrier between the hot confined plasma centre and the cold tokamak vessel. One of the fastest mechanisms of energy and particle loss from the confined plasma is turbulent transport.

One of the concepts to understand turbulence and its self–organization are zonal flows, further referred to as ZFs. ZFs have two branches, near-zero frequency flows and geodesic acoustic modes further referred to as GAMs with higher frequency(typically tens of kHz on most tokamaks of modest size and regular aspect ratio). The symmetry and stability of ZFs cause the energy of turbulence to flow out and thus, ZFs cause saturation of drift–wave turbulence [1].

A possible way to reduce turbulent transport in magnetically confined plasma is the stimulation of ZFs over their natural value via plasma edge potential biasing. There were conducted experiments with DC plasma potential biasing on several devices for magnetic plasma confinement, resulting in reduced radial transport [4], as well as experiments with time–varying potential biasing on the ISTTOK tokamak [9], during which GAMs were stimulated and that resulted in reduced radial transport as well.

During the preparation of previous thesis [5], similar experiments in the GOLEM tokamak and in the COMPASS tokamak were performed, where time–varying plasma edge potential biasing was applied. The goal of these experiments was stimulation of GAMs over their natural value.

To describe the impact of biasing on edge plasma, electrostatic Langmuir and Ball–pen probes were used. In the case of the COMPASS tokamak a probe head on fast reciprocating manipulator was used, allowing measurement of the whole profile during one shot. In the case of GOLEM tokamak a double rake of Langmuir probes (DRP) together with five–fold probe were used to measure edge plasma.

In the following work, further spectral analysis of data from the COMPASS

tokamak is presented in chapter 1.

In chapter 2, restoration of the DRP is described together with new features of the changed DRP manipulator, this restoration should lead to improved reliability of the DRP.

Chapter 3 describes the experiments performed in the GOLEM tokamak that should lead to GAM localization and characterization and the impact of GAM on turbulent transport.

Chapter 1

Spectral analysis of data from the COMPASS tokamak plasma biasing experiments

In the following chapter, further spectral analysis broadening the results from the previous thesis [5] are shown. The result of the previous thesis concerning data from COMPASS tokamak was a coherogram, obtained via wavelet transform, showing structures at the GAM oscillations frequency at the times when the right biasing frequency was applied. The more detailed analysis focuses on conditional averaging over biasing frequency together with a better distinction of GAM–like structures from the background.

1.1 Experimental setup

The impact of edge plasma potential biasing was examined in shots #17561 – #17564, where the biasing potential was applied using the lower second divertor tile, i.e., the plasma in those shots was in a limiter regime, limited by the divertor (Figure 1.1),$I_\mathrm{p} = 210$ kA,$n_\mathrm{e} = 4 \times 10^{19}$ m^{-3}). To make a scan in frequencies around the assumed GAM frequency, the waveform of biasing voltage was sweeping periodically with period T_sweep from f_low to f_high, these parameters for particular shots can be seen in Table 1.1.

Diagnostics used for the evaluation of the influence of biasing on the GAM were a ball-pen probe on the horizontal reciprocating manipulator for the

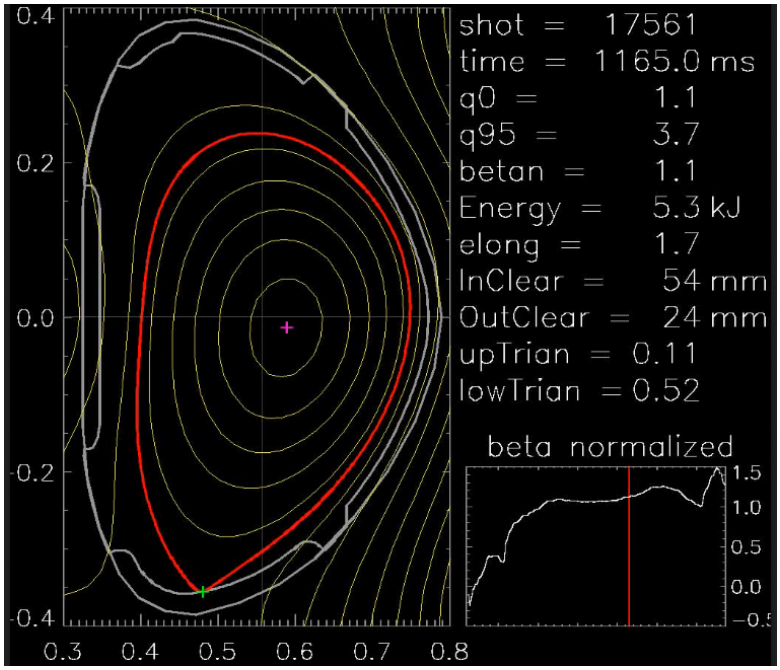

Figure 1.1: Reconstruction of flux surfaces from shot #17561, obtained via the EFIT code.

shot	f_{low}[kHz]	f_{high}[kHz]	T_{sweep}[ms]
#17561	20	40	10
#17562	20	40	10
#17563	20	40	1.5
#17564	2	8	5

Table 1.1: Parameters of applied biasing voltage for shots # 17561 – # 17564.

estimate of plasma potential ϕ, further referenced as BPP1_floating as it is the name of the signal in COMPASS database, and separatrix position R_{sep} from the EFIT magnetic reconstruction code. R_{sep} was corrected using radial position of ϕ maxima obtained from the position of the reciprocating manipulator. In the ϕ estimate, the influence of electron temperature T_{e} is neglected since T_{e} fluctuations are expected having a higher frequency.

Initially, the ϕ signal and the waveform of the biasing voltage were decimated by factor 5 to reduce the amount of processed data, resulting in a sampling frequency of 1 MHz. This decimation was justified by the fact, that according to the Nyquist – Shannon sampling theorem, the sampling frequency must be at least double of the highest frequency in the signal spectrum to avoid aliasing. Thus, 1 MHz sampling frequency gives 500 kHz of maximum frequency in spectra, which exceeds the frequency band (20 – 40 kHz) by factor 10. However, it was found later that it is necessary to use non–decimated data to obtain enough statistical samples for conditional averaging.

1.2 Spectral characteristics

Whereas the estimated frequency of GAM oscillations on COMPASS is ≈ 25 to 35 kHz [8], an electrostatic fluctuations of corresponding frequency were searched in the power spectra of floating potential ϕ. Power spectral densities were obtained as ensemble average during the movement of the probe through the plasma i.e. when the probe head was inside LCFS. The frequency resolution 97.5 Hz, given by the chosen window length of 2^{11} and sampling frequency 1 MHz, is a compromise between the adequate distinction of GAM–like oscillations peak width and excessively oscillating result.

As can be seen in Fig. 1.2, in the shot #17562, no oscillations of desired frequency were apparent in the signal, it was probably caused by the insufficient depth of probe insertion into the LCFS, because in limited plasma, GAM is localized deeper in the plasma [8].

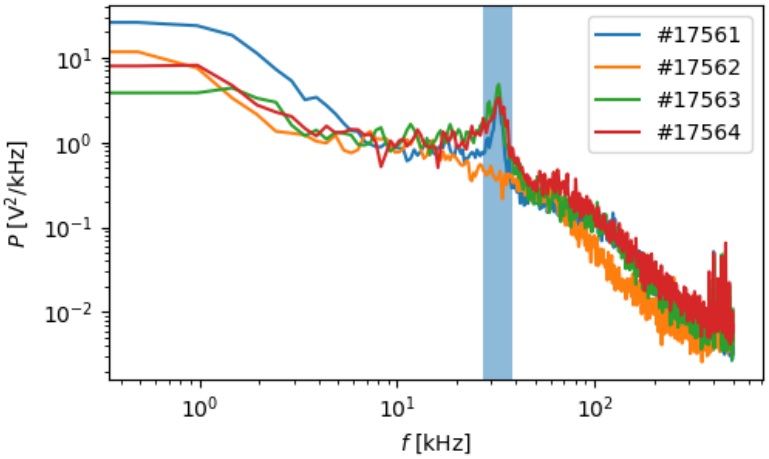

Figure 1.2: Power spectra of plasma potential inside LCFS. A sharp peak at about GAM–oscillations frequency of 32 kHz can be seen.

According to the Table 1.1 and Figure 1.2, the possible impact of biasing on GAM was examined in shots #17561 and #17563, where the voltage of correct biasing frequency was applied and where the probe was deep enough to see GAM. Shot #17564 was used as control shot with natural GAM occurrence only, because applied biasing voltage had frequency from 2 to 8 kHz, i.e., it was more likely to stimulate the near–zero frequency ZFs than GAMs.

1.3 Conditional averaging

To examine whether there was an impact of the biasing voltage on the mode and to reduce the effect of other quantities on the mode, conditional averaging over biasing frequency was applied. The goal is to characterize dependency of the BPP1_floating energy in given frequency band $E_{\mathrm{GAM}} = \mathrm{band-pass}(V_{\mathrm{fl}}, f_1, f_2)^2$, where f_1 and f_2 are lower and upper cutoff frequency respectively, on biasing frequency f_{BIAS}, i.e., to acquire

$$E_{\mathrm{GAM}} = E_{\mathrm{GAM}}\left(f_{\mathrm{BIAS}}\right).$$

First, BPP1_floating signal was band–passed with cut-off frequencies 27 and 38 kHz around expected GAM oscillations to observe only the frequency range of GAM.

Second, E_{GAM} characterizing power in the given frequency band (either Fourier transform, wavelet transform or square of BPP1_floating) was calculated. Then the data was split into groups given by the biasing frequency with the biasing frequency resolution of 1 kHz. (Technically, the sawtooth function representing the frequency sweep was evaluated in values of the E_{GAM} time axis, then the values were then rounded to integers.) In each frequency group, the mean of the value E_{GAM} was calculated.

Figure 1.3 shows a spectrogram obtained with a Fourier transform of shot #17561, where regions of interest are marked with orange. Selection of those areas was determined by the occurrence of GAM–like frequency oscillations. To obtain a comparable result from shots #17561 and #17563 and from the particular time windows, similar position of the probe towards the separatrix was further demanded as much as the same phase of probe movement, thus the area had to be shrunk (for the shot #17561 the window must be at least 10 ms long to count in all the biasing frequencies).

In the lower part of Figure 1.3, a spectrogram of biasing voltage is depicted, the sawtooth waveform of f_{BIAS} with the period of 10 ms is observable, together with a slight decrease in amplitude of biasing potential.

As can be seen in Figure 1.3 and Figure 1.4 there was an evident difference between the depth of probe insertion during shots #17561 and #17563. This difference resulted in the impossibility of finding time window, where all the above–mentioned conditions (GAM-like oscillations, comparable radial position and 10 ms window in shot #17561) could be kept. The final chosen windows were 1135 – 1145 ms for shot #17561, where the depth of insertion of the probe inside separatrix R_{p} went from -6.3 to -13.5 mm, and 1149 – 1154 ms for shot #17563, where R_{p} went from -11.2 to -12.5 mm. The reason for using only the data from probe insertion is, that during the backward movement of the probe, no significant rise of power in the given frequency band was observed a possible explanation of this behaviour could be that the plasma was perturbed by the probe itself.

No effect of biasing was seen neither in the middle period of reciprocating in

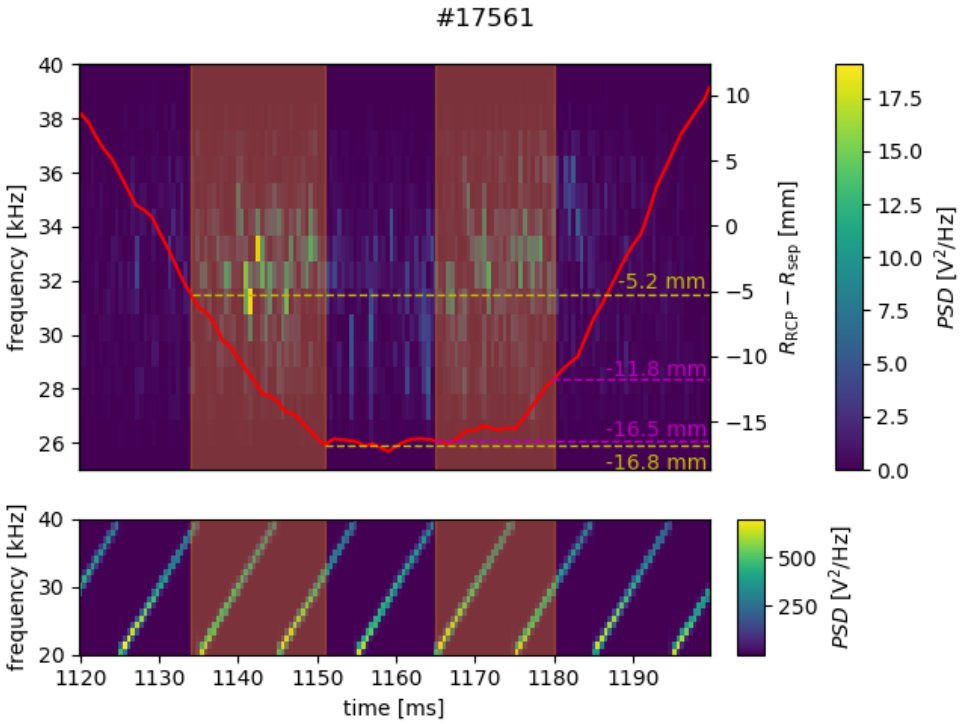

Figure 1.3: Spectrograms of the band–passed BPP1_floating signal and the biasing voltage from shot #17561, showing two regions with GAM candidate oscillations in time intervals 1138 to 1150 ms and 1169 to 1180 ms. Red line shows the position of the probe head toward the separatrix, dashed lines mark the radial position of GAM regions.

shot #17563, where the frequency of GAM–like oscillations slightly dropped from ≈ 33 kHz to ≈ 29 kHz. One could say that on one hand, the power of the signal was not raised because the probe was too deep in the plasma, where the plasma could not be affected by the biasing voltage applied at the plasma edge, on the other hand, this would be in contradiction to the results from shot #17561.

Fourier transform spectrogram was calculated with no segment overlap, to avoid statistical correlation, and window length of 2^{10} samples, allowing adequate frequency resolution. However, it appeared that although raw, non–decimated data was used, it was not possible to obtain enough samples for averaging as the maximum of 10 samples per one statistical ensemble could be obtained. On top of that, in most ensembles there was only 3 or 4 samples, which is not enough for a meaningful conditional averaging. Thus, the result of the Fourier transform spectrogram is not presented in this report.

Better frequency resolution for lower frequencies is provided by continuous

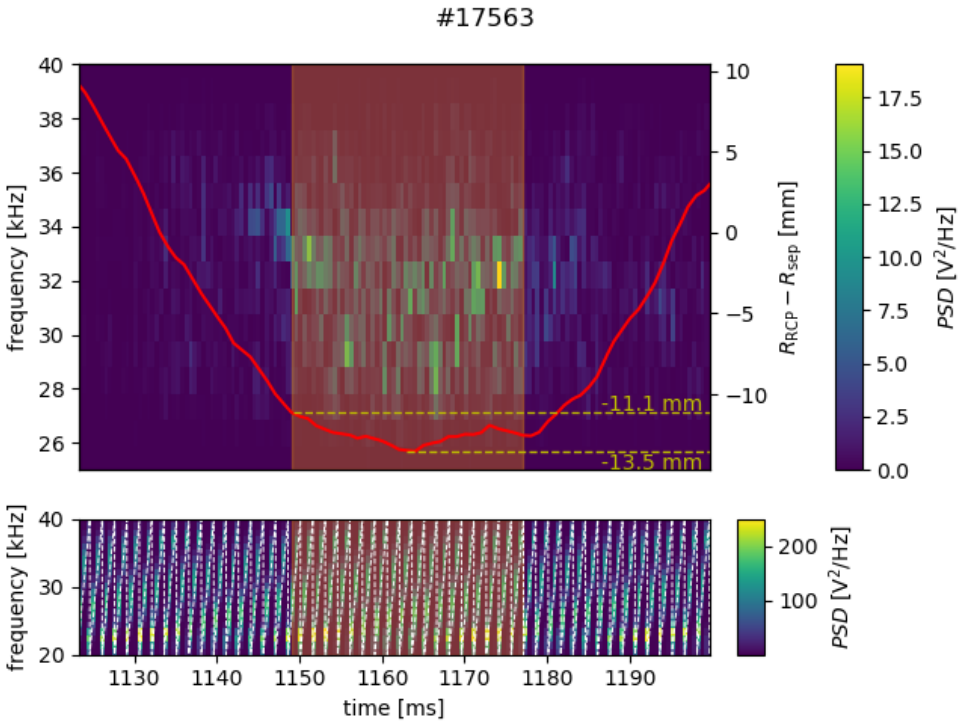

Figure 1.4: Spectrograms of the band–passed BPP1_floating signal and biasing voltage from shot #17563, where GAMs occurred in time interval from 1149 to 1177 ms. A decrease of GAM frequency is apparent when the probe is at the turning point.

wavelet transform, it was therefore used to compute the spectrogram of BPP1_floating signal too. Integral wavelet transform with the complex Morlet mother wavelet was used, which is a sine wave modulated by a Gauss function i.e. $e^{i\omega_0\nu-\frac{\nu^2}{2}}$, where ω_0 is nondimesional frequency and ν is a nondimensional time parameter [11].

Figure 1.5 shows results from conditional averaging, where continuous wavelet transformation was used to obtain time–frequency resolved spectra. There can be seen a rise of power in the GAM frequency oscillations in both shots at the times the right ($\approx$ 32 – 35 kHz) biasing frequency was applied. This result indicates that the GAM–like oscillations could have been affected by the biasing voltage, howbeit poor statistical significance could show that no conclusion can be made on the basis of wavelet spectrogram averaging. Thus, the statistical significance is resolved in the following paragraph.

Another mean to characterize the power of the signal in frequency band from 28 to 37 kHz was the square of the band–passed signal. For this approach, a statistical uncertainty of the result was determined by bootstrapping. The stationary bootstrap [7] method with a block length of 20 samples on average was used to generate 1000 samples of E_{GAM}. The block length is given by the time when auto-correlation function falls to 1/e to avoid having statistically correlated samples. Those samples were later used to characterize

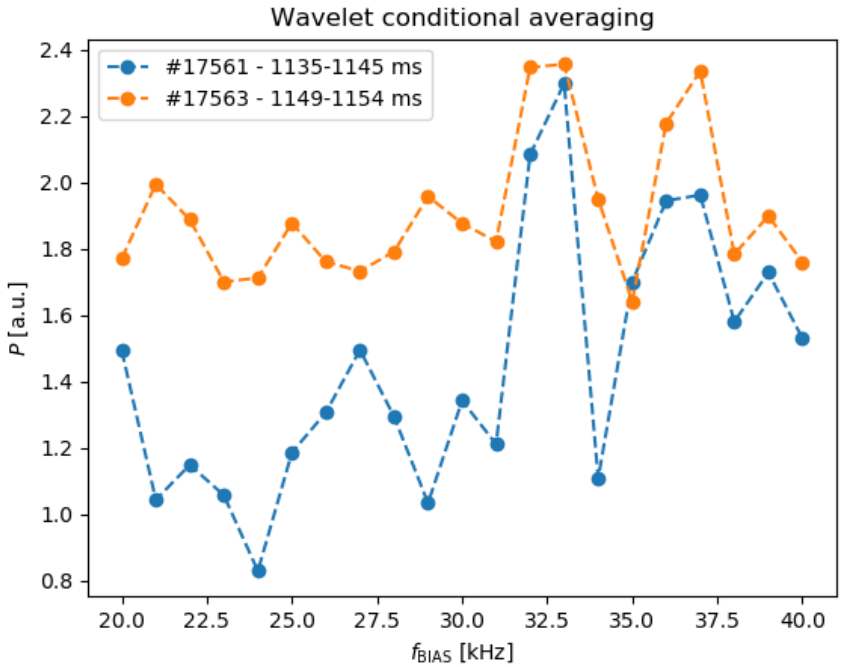

Figure 1.5: Wavelet transform of BPP1_floating in frequency range from 27 to 38 kHz depending on the biasing frequency f_{BIAS}.

the statistical distribution of conditionally averaged E_{GAM} via quantiles $q_{0.025}, q_{0.975}$ and $q_{0.5}$ (the median).

In Figure 1.5 and Figure 1.6, a good correspondence of trends indicating GAM oscillation stimulation computed with different methods can be seen. However, in Figure 1.6 it is apparent that at least in shot #17561 there was a growth of the GAM oscillations power when the f_{BIAS} was in accordance with the GAM oscillations frequency. However, this can be caused by the position of the probe and only one sweep of biasing voltage to be averaged by, as the growth of the power of GAM oscillations rose with the depth of insertion and with the f_{BIAS}. A different situation is in the shot #17563, where the duration of one sweep was 1.5 ms, therefore 4 sweeps were used for the averaging. As depicted in Figure 1.6 the median of the peak at 31 – 32 kHz is above the part of the graph, where the f_{BIAS} is low. In addition the $q_{0.025}$ of this peak is comparable to the $q_{0.975}$ of low f_{BIAS}. Based on these observations one can say that there was a statistically significant impact of the biasing on GAM oscillations, during the chosen time window in shot #17563.

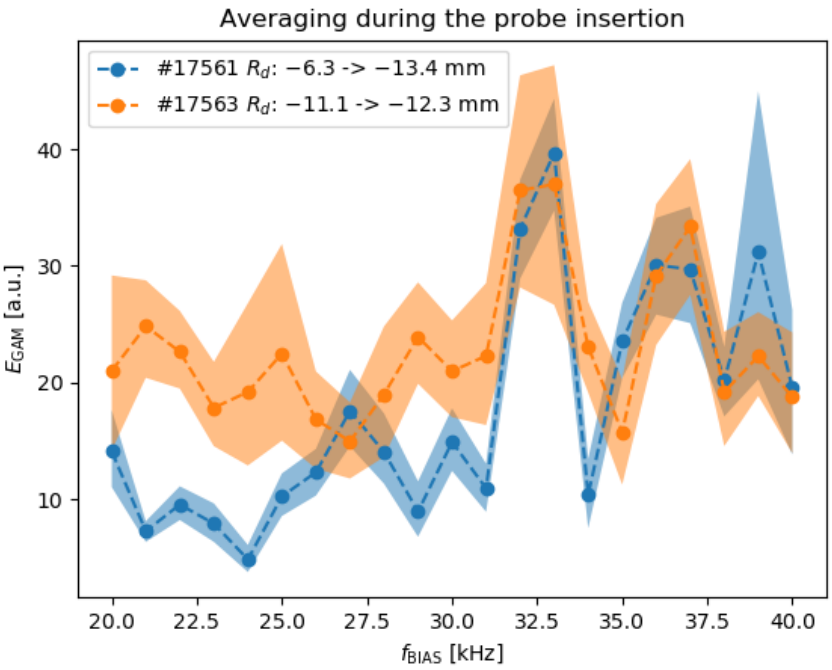

Figure 1.6: Power of band–passed signal

Chapter 2

DRP restoration on GOLEM tokamak

The unreliability of the double rake probe (DRP) head was a serious problem during measurements in the former thesis that led to multiple openings of tokamak vessel and delays. The main reasons of the DRP head malfunction were identified as old and thus fragile vacuum cables, improper pins and a probe manipulator that allowed fast movement of the probe and 360° rotational movement when the probe was inside the tokamak vessel. This movement could result in cable damage.

It was decided to replace all cables connecting the probe head and the vacuum bushing. A 25–pin D–sub connector was substituted by two 9–pin D–sub connectors (Figure 2.1a) to facilitate movement inside the narrow tokamak port, the metal part of each connector was also removed to reduce a chance of jamming.

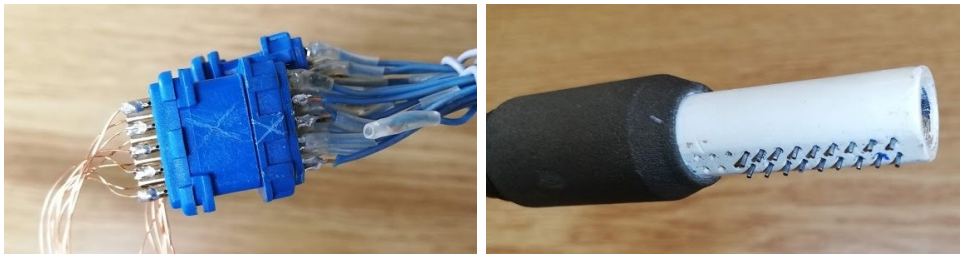

(a) : 9–pin D–sub connectors. **(b) :** Purged probe head with Mb pins.

Figure 2.1: New and repaired vacuum components of DRP head.

Old pins of unknown material properties were removed and new molybdenum–wire ones were installed during the work on the probe head. Those pins have

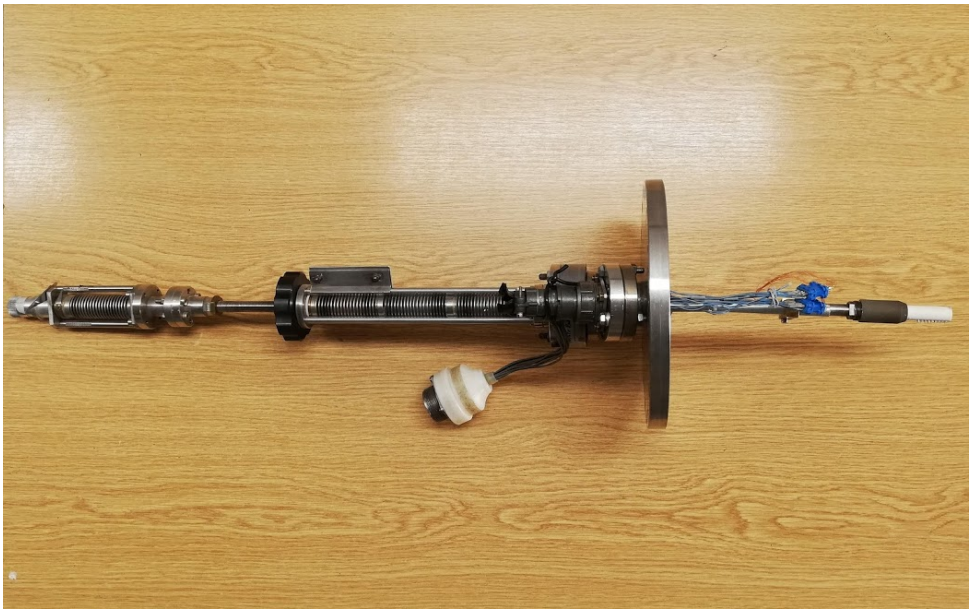

Figure 2.2: The DRP head on a more reliable manipulator.

a diameter of 0.75 mm and a length protruding above the surface of 1.5 mm. Radial distance of individual pins is 2.5 mm just as the poloidal distance. Spatial resolution during one shot is therefor 2.5 mm, but can be enhanced by moving the probe between shots.

The boron nitrite shielding was purged, as depicted in Figure 2.1b, of the first singed layer to reduce the possibility of spark creation.

To eliminate the possibility of cable rupture and to enable more precise movement of the probe, the probe had was placed on a different manipulator shown in Figure 2.2. This manipulator allows the placement of the probe head with a precision of 0.5 mm. Because a screw drive of the manipulator is used, the movement is slow in general but the usage is more convenient as only one hand is necessary for operation. Furthermore, the 360° rotational movement is now not possible, unless the probe is withdrawn from the tokamak vessel.

Chapter 3

Search for GAMs in the GOLEM tokamak

In order to facilitate the possible GAM stimulation in further experiments, series of long correlation radial measurements were performed to localize the GAM radially. The $n = 0$ toroidal symmetry and well approximated GAM frequency was exploited to localise the mode. To estimate the influence of present GAMs on tokamak, a fluctuation characterization of I_sat was performed.

3.1 Characterization of edge turbulence on GOLEM tokamak

To characterize edge turbulence on GOLEM tokamak, above mentioned DRP on moving manipulator was used. The probe was placed in the north–west lower port of the GOLEM tokamak. Special measurement module allows measurements of either floating potential V_{fl} using voltage divider 1:100 or ion saturation current I_{sat}, where individual pins are charged to -100 V. It is then possible to estimate electron density n_{e} neglecting the $\sqrt{T_{\mathrm{e}}}$ fluctuations [10].

The edge turbulence can be characterized by the moments of probability distribution function (PDS) of I_{sat} fluctuations , i.e., normalized standard deviation, skewness and curtosis.

The computation of the normalized standard deviation std_{norm} was follow-

ing

$$std_{\text{norm}} = \frac{\sqrt{\overline{|I_{\text{sat}} - \overline{I_{\text{sat}}}|^2}}}{\overline{I_{\text{sat}}}}, \tag{3.1}$$

where the vertical line denotes mean in time in this case. Normalized standard deviation std_{norm} describes the rate of turbulent flow.

The skewness is computed as the Fisher–Pearson [6] coefficient of skewness

$$skew_{\text{coef}} = \frac{m_3}{m_2^{2/3}}, \tag{3.2}$$

where m_{i} is the i–th central moment. The skewness characterize whether there was more positive or more negative fluctuations, i.e. whether a blob leaving plasma is measured, it is positive fluctuation, on the other hand when a hole passes the probe it is measured as negative fluctuation [2]. The skewness of the Gauss distribution is 0.

Eventually the kurtosis is a characteristics of PDF tail, in other words, it describes how wide the PDF is. From a physical point of view, if the kurtosis, defined by Fisher, is larger than 0 it indicates that turbulent structures passed around the probe.

In the following paragraphs, radial profiles of mean, normalized standard deviation, skewness and kurtosis from shots #33772, #33774, #33776, #33779, #33781 will be presented. The moments are calculated in time from 10 to 12 s, where a flat–top of the plasma current is localized.

In the Figure 3.1a a redial profile of I_{sat} can be seen. It is apparent that the mean is not rising towards the plasma center as expected, which could be a result of inadequate ground of the probe to the vessel. Another unexpected feature of the mean are negative values, but this could also be due to the inadequate ground. On the other hand, the small values of the signal are caused by known resistor in the measurement module.

Tiny and negative values of mean result in negative and high normalized standard deviation in Figure 3.1b.

On the contrary, profiles of the skewness (Figure 3.1c) and kurtosis (Figure 3.1d) roughly correspond with the expected profiles. These moments should be a subject of further investigation as the mean and normalized standard deviation does not agree with former experiments executed in the GOLEM tokamak.

3.2 Pursuit of GAMs

There are two important features of GAM that were used to localize the mode in the edge plasma of the GOLEM tokamak:

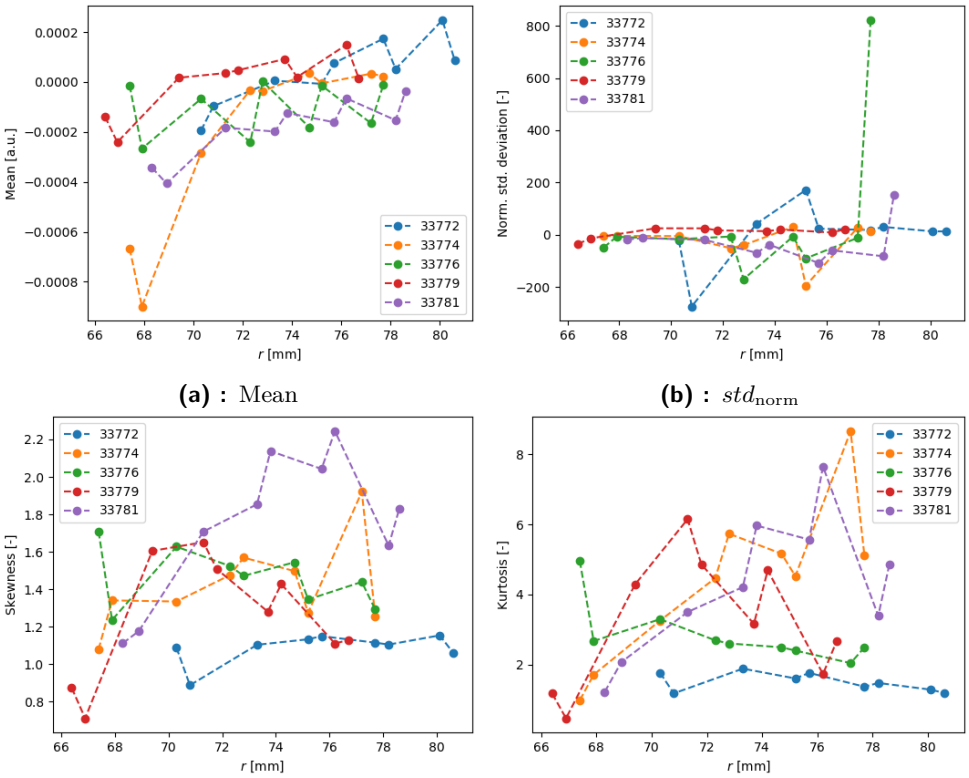

(a) : Mean **(b) :** std_{norm}

(c) : Skewness **(d) :** Kurtosis

Figure 3.1: Moments of PDF of I_{sat} fluctuations.

1. In the circular plasma the following approximation of GAM frequency f_{GAM} can be used

$$f_{\text{GAM}} = \frac{c_{\text{s}}}{2\pi R}, \tag{3.3}$$

where c_{s} is the sound velocity in plasma and R is the major radius of the tokamak [9].

2. As a branch of ZFs, GAMs have $n = 0$ in density and potential.

The f_{GAM} was estimated as $f_{\text{GAM}} \approx 10 - 15$ kHz using following $c_{\text{s}} = \sqrt{11600 \cdot k_{\text{b}} \cdot T_{\text{e}}/M}$, where k_{b} is Boltzmann constant T_{e} is electron temperature in eV and M is the mass of proton, T_{e} was in the GOLEM tokamak earlier estimated here [3]. Frequencies around the estimate were later searched for in the spectra of either V_{fl} or I_{sat}.

The symmetrical nature of GAMs was exploited in the following manner. As the toroidal mode number n of GAM is zero, it should be possible to observe the GAM oscillations on two separate toroidal positions with virtually no lag between them within the measurement precision and 0 cross–phase. To conduct simultaneous measurements of V_{fl} and I_{sat}, apart from DRP a five–fold probe was used. On Figure 3.2 the scheme of probes placement can

be seen, reflecting the real spatial layout of the probes.

Besides the $n = 0$ symmetry in density and potential, GAMs have poloidal

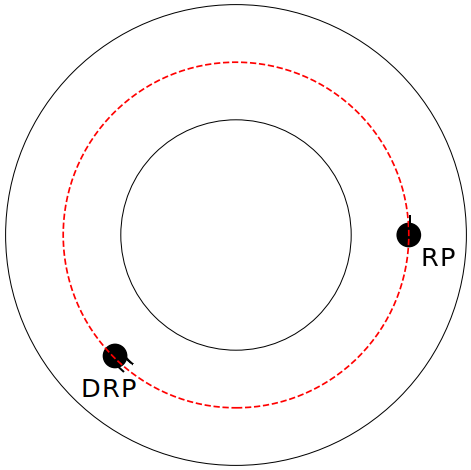

Figure 3.2: Scheme of probes placement for measurements of GAM oscillations toroidal symmetry.

mode number $m = 0$ in potential and $m = 1$ in density, nevertheless investigation of this property was not realized in the experimental part of this work, because ob the probes were placed in the lower ports of the GOLEM tokamak. It could be done in future, maybe even three position simultaneous measurements could be executed.

To find a GAM in the DRP and five–fold probe signals, cross methods of signal processing were used.

First, a GAM candidate had to be found, for this purpose a wavelet coherogram, like in Figure 3.3, was used as it enabled a fast identification of the GAM–like frequency oscillations that were apparent in the signal of both DRP and five–fold probe. As the time window of the GAM candidate was estimated from the coherogram, Fourier transform coherence averaged over the whole time window was calculated. Since the used coherence is a value derived from cross-spectrum that involves information about the cross–phase. A resemblance of two signals can be estimated via value absolute of coherence and cross–phase. Toroidally symmetrical GAMs should show high absolute value of coherence and at the same time 0 cross phase.

During the measurements, the position of both probes was setup the way that the deepest pin on the DRP was at the same assumed flux surface as the ball–pen probe and the Langmuir probe on the five–fold probe. Thus, when the long correlation measurements were evaluated, it was always between the deepest pin on the DRP and five–fold probe.

To search the GAMs only in steady state regime called 'flat–top' a simple algorithm of 'flat–top' detection in the GOLEM tokamak was established. This algorithm found the maximum I_{max} of the plasma current I_{pl} and then chose only those parts of signal where the I_{pl} was at least 95% I_{max}. Two series of measurements of V_{fl} with the DRP and the ball–pen probe were

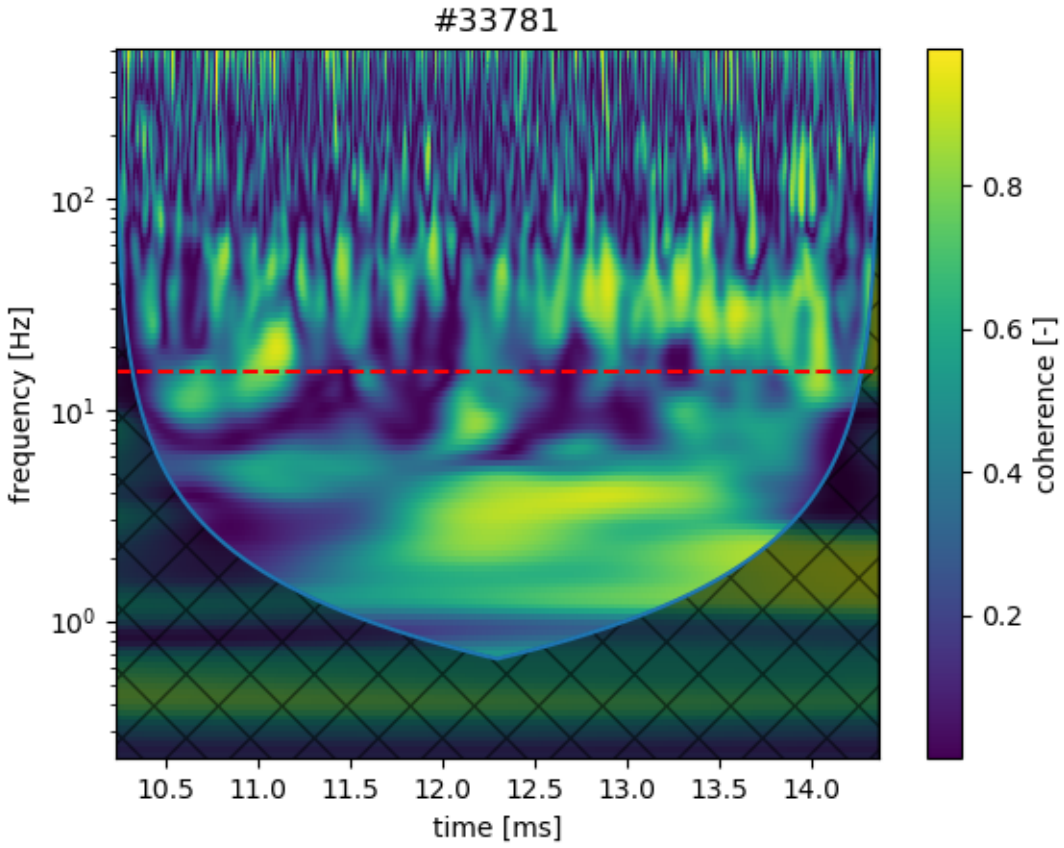

Figure 3.3: Wavelet coherogram with a GAM candidate in time interval 10.8 – 11.1 ms.

performed, one was oriented to make a profile of V_{fl} (shots #33469 – #33493, $U_{\text{CD}} = 450$ V, $U_{\text{B}_\text{t}} = 800$ V and $p^{\text{request}} = 10$ mPa) and localize the GAM radially. The other V_{fl} session was scan through parameters of plasma discharge on GOLEM (shots #33659 – #33702) to find a regime where GAM would occur. During the plasma paremeters scan session, pressures from 5 to 20 mPa with step of 5 mPa were tried. Then the pressure was fixed to 15 mPa and the U_{CD} was varied from 220 to 650 V and U_{B_t} was varied from 450 to 1000 V.

There was also one session of I_{sat} measurements (shots #33769 – #33799, $U_{\text{CD}} = 450$ V, $U_{\text{B}_\text{t}} = 800$ V and $p^{\text{request}} = 10$ mPa) with the DRP and the Langmuir probe on the five–fold probe. However in no discharge the GAMs were found, which is illustrated in Figure 3.4.

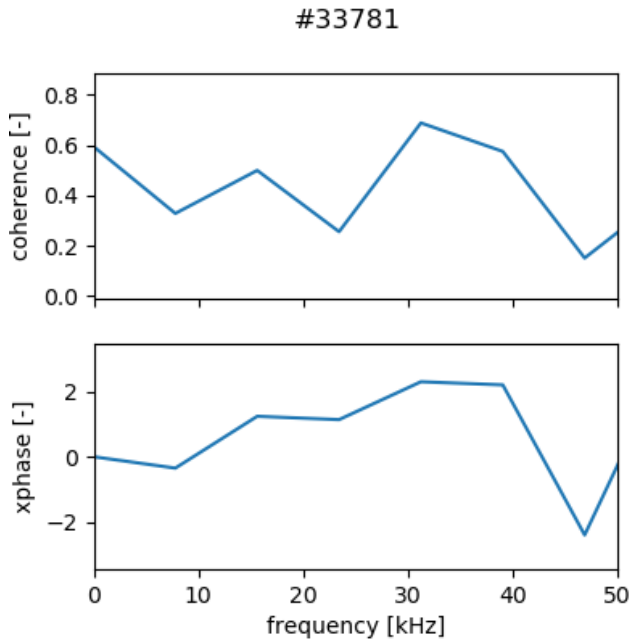

Figure 3.4: Illustration of the GAM absence in the shot #33781. So that one can say that there was the GAM, the cross–phase would have to be around zero and the value absolute would have to exceed 0.7 or better 0.8 in the expected GAM frequency region.

Chapter 4

Conclusion

The possible impact of time–varying potential biasing on GAM was examined in the COMPASS tokamak. Conditional averaging over the biasing frequency showed that there was a statistically significant impact of the biasing voltage during the shot #17563. The four sweeps provide a good basis that other effects did not affect the result. On the other hand, the result from shot #17561 that show statistically much more significant impact of the biasing voltage on the GAM could have been affected much easier as only one sweep of biasing voltage was counted in the averaging. As can be seen in Figure 1.3 and in Figure 1.4 the GAM oscillations change its nature during one shot considerably, in the shot #17561 no oscillations of GAM–like frequency were observed and in the shot #17563 the frequency of the oscillations has fallen in when the probe was at the turning point.

Further, no impact was seen during the returning phase of the probe neither in the shot #17561 nor #17563, despite the fact that the probes were moving thought the same position towards the separatrix. This could be caused by the fact that the plasma was perturbed by the probe itself.

It is interesting that GAM oscillations with expected frequency of ≈ 32 – 35 kHz were observed deeper in the plasma in the shot #17561 than in the shot #17563 and it could even be impacted by the biasing voltage. However, no impact of biasing voltage on GAM oscillations was observed in the middle part of the reciprocation during the shot #17563, thus it is a possible way of future research to estimate the maximal depth where plasma could be affected by divertor biasing.

Despite executed experiments in the GOLEM tokamak, no evidence of the GAMs was found. This can be caused by many reasons.

A regime of plasma in the GOLEM tokamak, where GAMs occur, exists but was not tried or the probe pair was not at the right radial position to measure the GAM. Since the radial profile of V_{fl} was performed for only one

discharge settings and during the scan of plasma parameters only one radial position was observed by both the probes, there is a possibility that the GAM was missed. A second rake of Langmuir probes on separate manipulator would facilitate the long range correlation measurements as more radial positions could be observed by both the probes at once.

Perhaps the plasma of GOLEM tokamak is not hot enough and the gradients are not steep enough for the turbulence to fully emerge. And as ZFs take the energy from turbulence, no ZFs can emerge either. One shot in the GOLEM tokamak is $\approx$ 10 ms long, maybe a longer shots could provide the background for GAM observation. Plasma stabilization could improve the results significantly.

The main motivation to measure the turbulence was characterization of GAM impact on the turbulence. However, in view of the fact that no evidence of the GAMs was found, unsuccessful characterization of turbulence in the edge plasma is not an issue at the time. In future experiments the ability to characterize turbulence is going to be irreplaceable.

Bibliography

[1] Fujisawa, A. A review of zonal flow experiments. *Nuclear Fusion 49*, 1 (dec 2008), 013001.

[2] Manz, P., Ribeiro, T. T., Scott, B. D., Birkenmeier, G., Carralero, D., Fuchert, G., Müller, S. H., Müller, H. W., Stroth, U., and Wolfrum, E. Origin and turbulence spreading of plasma blobs. *Physics of Plasmas 22*, 2 (2015), 022308.

[3] Mácha, P. Měření základních parametrů okrajového plazmatu pomocí kombinované ball-pen a langmuirovy sondy na tokamaku golem, 2018.

[4] Oost, G. V., mek, J. A., Antoni, V., Balan, P., Boedo, J. A., Devynck, P., uran, I., Eliseev, L., Gunn, J. P., Hron, M., Ionita, C., Jachmich, S., Kirnev, G. S., Martines, E., Melnikov, A., Schrittwieser, R., Silva, C., ckel, J. S., Tendler, M., Varandas, C., Schoor, M. V., Vershkov, V., and Weynants, R. R. Turbulent transport reduction byE bvelocity shear during edge plasma biasing: recent experimental results. *Plasma Physics and Controlled Fusion 45*, 5 (mar 2003), 621–643.

[5] Papoušek, F. Impact of swept edge plasma potential biasing on turbulence in tokamaks. B.s. thesis, FNSPE CTU in Prague, 2019.

[6] Pearson, K. Contributions to the mathematical theory of evolution. ii. skew variation in homogeneous material. *Philosophical Transactions of the Royal Society of London. A 186* (1895), 343–414.

[7] Politis, D. N., and Romano, J. P. The stationary bootstrap. *Journal of the American Statistical Association 89*, 428 (1994), 1303–1313.

[8] Seidl, J., Krbec, J., Hron, M., Adamek, J., Hidalgo, C., Markovic, T., Melnikov, A., Stockel, J., Weinzettl, V., Aftanas, M., Bilkova, P., Bogar, O., Bohm, P., Eliseev, L., Hacek, P., Havlicek, J., Horacek, J., Imrisek, M., Kovarik, K., Mitosinkova, K., Panek, R., Tomes, M., and Vondracek, P. Electromagnetic characteristics of geodesic acoustic mode in the COMPASS tokamak. *Nuclear Fusion 57*, 12 (oct 2017), 126048.

[9] Silva, C., Henriques, R., Hidalgo, C., and Fernandes, H. Experimental evidence of turbulence regulation by time–varying $e \times b$ flows. *Nuclear Fusion 58*, 2 (dec 2017), 026017.

[10] Stöckel, J., Adamek, J., Balan, P., Bilyk, O., Brotankova, J., Dejarnac, R., Devynck, P., Duran, I., Gunn, J. P., Hron, M., Horacek, J., Ionita, C., Kocan, M., Martines, E., Panek, R., Peleman, P., Schrittwieser, R., Oost, G. V., and Zacek, F. Advanced probes for edge plasma diagnostics on the CASTOR tokamak. *Journal of Physics: Conference Series 63* (apr 2007), 012001.

[11] Torrence, C., and Compo, G. P. A practical guide to wavelet analysis. *Bulletin of the American Meteorological Society 79* (1998), 61–78.